On the Reaction Mechanism of Adduct Formation in LOV Domains of the Plant Blue-Light Receptor Phototropin

Erik Schleicher,[†] Radoslaw M. Kowalczyk,[†] Christopher W. M. Kay,[†]
Peter Hegemann,[‡] Adelbert Bacher,[§] Markus Fischer,[§] Robert Bittl,[†]
Gerald Richter,[§] and Stefan Weber*,[†]

*Contribution from the Institut für Experimentalphysik, Freie Universität Berlin, Arnimallee 14,
14195 Berlin, Germany; Institut für Biochemie I, Universität Regensburg, Universitätsstrasse 31,
93053 Regensburg, Germany; and Institut für Organische Chemie und Biochemie, Technische
Universität München, Lichtenbergstrasse 4, 85747 Garching, Germany*

Received January 26, 2004; E-mail: Stefan.Weber@physik.fu-berlin.de

Abstract: The blue-light sensitive photoreceptor, phototropin, is a flavoprotein which regulates the phototropism response of higher plants. The photoinduced triplet state and the photoreactivity of the flavin-mononucleotide (FMN) cofactor in two LOV domains of *Avena sativa*, *Adiantum capillus-veneris*, and *Chlamydomonas reinhardtii* phototropin have been studied by time-resolved electron paramagnetic resonance (EPR) and UV−vis spectroscopy at low temperatures ($T \leq 80$ K). Differences in the electronic structure of the FMN as reflected by altered zero-field splitting parameters of the triplet state could be correlated with changes in the amino acid composition of the binding pocket in wild-type LOV1 and LOV2 as well as in mutant LOV domains. Even at cryogenic temperatures, time-resolved EPR experiments indicate photoreactivity of the wild-type LOV domains, which was further characterized by UV−vis spectroscopy. Wild-type LOV1 and LOV2 were found to form an adduct between the FMN cofactor and the functional cysteine with a yield of 22% and 68%, respectively. The absorption maximum of the low-temperature photoproduct of wild-type LOV2 is red-shifted by about 15 nm as compared with the FMN C(4a)-cysteinyl adduct formed at room temperature. In light of these observations, we discuss a radical-pair reaction mechanism for the primary photoreaction in LOV domains.

Introduction

Blue and near-ultraviolet light regulates essential physiological processes in a wide range of organisms. In plants, blue-light responses include stem bending toward a light source (phototropism), chloroplast migration to places of appropriate light intensity (chloroplast photorelocation), and the opening of stomatal guard cells to facilitate gas exchange. In green algae, blue light plays a further central role in controlling the progression of their sexual life cycle. The photoreceptors involved in these processes are the plasma membrane-associated phototropins and homologues, which are encoded by the phot genes.[1−9] The common features of the phototropin photoreceptor family are two light-sensitive domains, LOV1 and LOV2,[10,11] in the N-terminal part of each protein and a C-terminal serine/threonine kinase domain. Each of the two LOV domains noncovalently binds a single flavin mononucleotide (FMN) as a chromophore.[11]

After illumination by blue light, recombinant LOV domains of plant and algal phot-proteins undergo a transient and fully reversible bleaching of their optical absorptions at 400−500 nm[11] accompanied by a bathochromic shift of the band at 370 nm to 390 nm.[12−14] Based on the similarity of the 390-nm band in LOV2-390[12] (see Figure 1) with that of a functional intermediate in mercuric ion reductase,[15] it was suggested that the LOV photocycle comprises a light-induced addition of a thiol group to the C(4a) position of the FMN chromophore. This hypothesis has been confirmed by NMR studies of the light-

[†] Freie Universität Berlin.
[‡] Universität Regensburg.
[§] Technische Universität München.

(1) Briggs, W. R.; Christie, J. M. *Trends Plant Sci.* **2002**, *7*, 204.
(2) Kagawa, T. *J. Plant Res.* **2003**, *116*, 77.
(3) Christie, J. M.; Reymond, P.; Powell, G. K.; Bernasconi, P.; Raibekas, A. A.; Liscum, E.; Briggs, W. R. *Science* **1998**, *282*, 1698.
(4) Kagawa, T.; Sakai, T.; Suetsugu, N.; Oikawa, K.; Ishiguro, S.; Kato, T.; Tabata, S.; Okada, K.; Wada, M. *Science* **2001**, *291*, 2138.
(5) Sakai, T.; Kagawa, T.; Kasahara, M.; Swartz, T. E.; Christie, J. M.; Briggs, W. R.; Wada, M.; Okada, K. *Proc. Natl. Acad. Sci. U.S.A.* **2001**, *98*, 6969.
(6) Kinoshita, T.; Doi, M.; Suetsugu, N.; Kagawa, T.; Wada, M.; Shimazaki, K.-i. *Nature (London)* **2001**, *414*, 656.
(7) Briggs, W. R.; Beck, C. F.; Cashmore, A. R.; Christie, J. M.; Hughes, J.; Jarillo, J. A.; Kagawa, T.; Kanegae, H.; Liscum, E.; Nagatani, A.; Okada, K.; Salomon, M.; Rüdiger, W.; Sakai, T.; Takano, M.; Wada, M.; Watson, J. C. *Plant Cell* **2001**, *13*, 993.
(8) Crosson, S.; Rajagopal, S.; Moffat, K. *Biochemistry* **2003**, *42*, 2.
(9) Huang, K.; Beck, C. F. *Proc. Natl. Acad. Sci. U.S.A.* **2003**, *100*, 6269.
(10) Huala, E.; Oeller, P. W.; Liscum, E.; Han, I.-S.; Larsen, E.; Briggs, W. R. *Science* **1997**, *278*, 2120.
(11) Christie, J. M.; Salomon, M.; Nozue, K.; Wada, M.; Briggs, W. R. *Proc. Natl. Acad. Sci. U.S.A.* **1999**, *96*, 8779.
(12) Salomon, M.; Christie, J. M.; Knieb, E.; Lempert, U.; Briggs, W. R. *Biochemistry* **2000**, *39*, 9401.
(13) Swartz, T. E.; Corchnoy, S. B.; Christie, J. M.; Lewis, J. W.; Szundi, I.; Briggs, W. R.; Bogomolni, R. A. *J. Biol. Chem.* **2001**, *276*, 36493.
(14) Kottke, T.; Heberle, J.; Hehn, D.; Dick, B.; Hegemann, P. *Biophys. J.* **2003**, *84*, 1192.
(15) Miller, S. M.; Massey, V.; Ballou, D.; Williams, C. H.; Distefano, M. D.; Moore, M. J.; Walsh, C. T. *Biochemistry* **1990**, *29*, 2831.
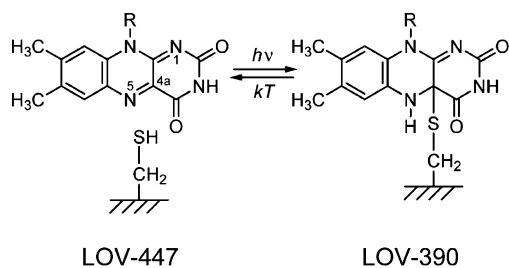
Figure 1. Photoreaction of LOV domains.

induced differences in the chemical shifts of various ^{13}C/^{15}N-labeled isotopologs of FMN bound to the LOV2 domain of *Avena sativa*[16] (oat) and later-on also by X-ray crystallography of a LOV2 domain from *Adiantum capillus-veneris* (maidenhair fern)[17] and a LOV1 domain from *Chlamydomonas reinhardtii* LOV1.[18] The reactive cysteine is C450 in *A. sativa* and C966 in *A. capillus-veneris* LOV2 domains and C57 and C250 in *C. reinhardtii* LOV1 and LOV2 domains,[8,19] respectively. At room temperature in the dark, the photoproduct reverts to the ground state, LOV-447 (see Figure 1), on the time scale of minutes,[12,13,20] with a pH- and salt-concentration-dependent time constant.[14,21]

Despite some progress made in the understanding of the overall photoreaction of LOV domains, important mechanistic and conformational steps of their photocycle remain to be elucidated. The commonly accepted primary photophysical and photochemical reactions in the LOV domains involve intersystem crossing (ISC) from the singlet-excited state of the FMN chromophore to its triplet-excited state ($S_1 \rightarrow T_1$). In LOV2 this step has a quantum yield of $\Phi_T = 0.6-0.88$,[13,22,23] and a rate of $k_{ISC} = (2.7-3.3$ ns$)^{-1}$.[22,23] In *C. reinhardtii* LOV1 the FMN triplet is formed with a quantum yield of $\Phi_T = 0.23$ and at a rate of $k_{ISC} = (3.5$ ns$)^{-1}$ (assuming negligible excited singlet deactivation by internal conversion).[24] Once the FMN is in the triplet state, the subsequent mechanistic steps of adduct formation are still unclear. Several mechanisms for photoadduct formation have been suggested, all of which await experimental confirmation. Initially, an ionic mechanism relying on a deprotonated functional cysteine was proposed,[13] in which protonation of triplet-state FMN at N(5) by an unidentified proton-donating residue leads to an FMN cation which is subsequently attacked at the formally positive charged C(4a) by the thiolate anion. However, it has been shown by infrared (IR) spectroscopy on LOV2 from *A. capillus-veneris* Phy3[25] and on LOV1 from *C. reinhardtii* Phot1[26] that the reactive cysteines are protonated in the dark state. Subsequently, a

modified reaction scheme was presented, in which base abstraction of the thiol proton by the excited FMN is followed by a nucleophilic attack of the sulfide.[8] Finally, a concerted mechanism was proposed where the N(5) position of the FMN triplet is protonated as the thiol sulfur attacks C(4a).[27]

In all these suggested pathways, the important step of triplet-to-singlet-state conversion required for covalent-bond formation is only inadequately discussed. This shortcoming together with the fact that photoexcited flavins are potent oxidants for redox-active amino acid residues[28−30] has led to the proposal of a radical mechanism in which an FMN radical is formed by either electron abstraction or hydrogen-atom abstraction from the reactive cysteine by the FMN in the triplet state.[31,32] Thereby, a radical pair in the triplet-spin configuration is generated. This radical pair can easily convert to a singlet-spin configuration, which opens up the reaction channel for the FMN semiquinone to react with the cysteinyl radical to form the covalent thio-adduct, LOV-390. A radical-pair mechanism has further been found compatible with the observed stable chromophore−protein adduct which occurs upon illumination and subsequent thermal treatment of a LOV1 mutant in which the reactive C57 is replaced by methionine.[33,34] However, no radical-pair species have so far been observed in photoexcited wild-type LOV domains.

Regardless of which mechanism for photoadduct formation in LOV domains is correct, the FMN triplet is an important reactive intermediate which to date is only insufficiently characterized by spectroscopic techniques. To fill this gap, we have performed time-resolved electron paramagnetic resonance (EPR) spectroscopy on various photoexcited wild-type and mutant LOV domains. As we will show, such experiments do reveal important information not only on the global electron-spin distribution in the FMN triplet but also on its protonation state. Furthermore, information on the $S_1 \rightarrow T_1$ conversion is obtained from the fractional populations of the triplet sublevels, which were extracted from spectral simulations of the observed electron-spin polarization pattern of the EPR spectrum. Together with results from optical absorption experiments, which have been obtained under similar experimental conditions, a detailed picture of the photophysics of triplet formation and decay in LOV domains is presented.

Materials and Methods

Sample Preparation. Protein samples were prepared as described previously.[14,32] All recombinant LOV domains were initially isolated in a pH 8.0 buffer containing 10 mM sodium phosphate and 10 mM NaCl. Prior to the experiments, glycerol was added to a final

(16) Salomon, M.; Eisenreich, W.; Dürr, H.; Schleicher, E.; Knieb, E.; Massey, V.; Rüdiger, W.; Müller, F.; Bacher, A.; Richter, G. *Proc. Natl. Acad. Sci. U.S.A.* **2001**, *98*, 12357.
(17) Crosson, S.; Moffat, K. *Plant Cell* **2002**, *14*, 1067.
(18) Fedorov, R.; Schlichting, I.; Hartmann, E.; Domratcheva, T.; Fuhrmann, M.; Hegemann, P. *Biophys. J.* **2003**, *84*, 2474.
(19) Huang, K.; Merkle, T.; Beck, C. F. *Physiol. Plant.* **2002**, *115*, 613.
(20) Kasahara, M.; Swartz, T. E.; Olney, M. A.; Onodera, A.; Mochizuki, N.; Fukuzawa, H.; Asamizu, E.; Tabata, S.; Kanegae, H.; Takano, M.; Christie, J. M.; Nagatani, A.; Briggs, W. R. *Plant Physiol.* **2002**, *129*, 762.
(21) Corchnoy, S. B.; Swartz, T. E.; Lewis, J. W.; Szundi, I.; Briggs, W. R.; Bogomolni, R. A. *J. Biol. Chem.* **2003**, *278*, 724.
(22) Kennis, J. T. M.; Crosson, S.; Gauden, M.; van Stokkum, I. H. M.; Moffat, K.; van Grondelle, R. *Biochemistry* **2003**, *42*, 3385.
(23) Schüttrigkeit, T. A.; Kompa, C. K.; Salomon, M.; Rüdiger, W.; Michel-Beyerle, M. E. *Chem. Phys.* **2003**, *294*, 501.
(24) Islam, S. D. M.; Penzkofer, A.; Hegemann, P. *Chem. Phys.* **2003**, *291*, 97.
(25) Iwata, T.; Tokutomi, S.; Kandori, H. *J. Am. Chem. Soc.* **2002**, *124*, 11840.
(26) Ataka, K.; Hegemann, P.; Heberle, J. *Biophys. J.* **2003**, *84*, 466.

(27) Crosson, S.; Moffat, K. *Proc. Natl. Acad. Sci. U.S.A.* **2001**, *98*, 2995.
(28) Heelis, P. F.; Parsons, B. J.; Phillips, G. O. *Biochim. Biophys. Acta* **1979**, *587*, 455.
(29) Weber, S.; Kay, C. W. M.; Mögling, H.; Möbius, K.; Hitomi, K.; Todo, T. *Proc. Natl. Acad. Sci. U.S.A.* **2002**, *99*, 1319.
(30) Zhong, D.; Zewail, A. H. *Proc. Natl. Acad. Sci. U.S.A.* **2001**, *98*, 11867.
(31) Kay, C. W. M.; Kuppig, A.; Schleicher, E.; Bacher, A.; Richter, G.; Weber, S. Photochemistry of a C450A mutant of the LOV2 domain in phototropin: detection of a light-induced neutral flavin radical by EPR spectroscopy. In *Flavins and Flavoproteins 2002*; Chapman, S., Perham, R., Scrutton, N., Eds.; Rudolf Weber Agency for Scientific Publications: Berlin, 2002; p 707.
(32) Kay, C. W. M.; Schleicher, E.; Kuppig, A.; Hofner, H.; Rüdiger, W.; Schleicher, M.; Fischer, M.; Bacher, A.; Weber, S.; Richter, G. *J. Biol. Chem.* **2003**, *278*, 10973.
(33) Bittl, R.; Kay, C. W. M.; Weber, S.; Hegemann, P. *Biochemistry* **2003**, *42*, 8506.
(34) Kottke, T.; Dick, B.; Fedorov, R.; Schlichting, I.; Deutzmann, R.; Hegemann, P. *Biochemistry* **2003**, *42*, 9854.

concentration of 60% (v/v) to yield a transparent glass in the frozen state. The concentrations of the protein samples were adjusted to $\sim$0.7 mM using 10-kDa centrifugal concentrators (Millipore, Billerica, MA). Protein concentrations were controlled by optical absorption spectroscopy (ϵ_{447} = 13 800 M^{-1}cm^{-1} for *C. reinhardtii* LOV1[20] and *A. sativa* LOV2[12] and ϵ_{447} = 11 200 M^{-1}cm^{-1} for *A. capillus-veneris* LOV2) using a Shimadzu UV-1601PC (Shimadzu Scientific Instruments, Columbia, MD) spectrophotometer. All samples were then deoxygenated, transferred into EPR suprasil quartz tubes (3 mm inner diameter) under an argon atmosphere, and rapidly frozen in liquid nitrogen in the dark. For the low-temperature UV−vis experiments, the samples were transferred into optical cuvettes with a path length of 10 mm.

EPR Instrumentation. Time-resolved (tr) EPR experiments were performed using a laboratory-built spectrometer consisting of an AEG electromagnet, a Bruker ER041 MR (Rheinstetten, Germany) microwave bridge in conjunction with a Bruker ER4118X-MD-5W1 dielectric resonator, which was immersed in a laboratory-built helium-gas flow cryostat. The temperature of the sample was controlled to ±1 K by a LakeShore Cryotronics 321 (Westerville, OH) autotuning temperature controller. The microwave (mw) frequency was measured by an EIP 548 (Milpitas, CA) frequency counter, and the magnetic field, by a Bruker ER035 MR NMR gaussmeter. The time-dependent EPR signal elicited by pulsed laser excitation was amplified in a fast low-noise preamplifier and detected directly without magnetic-field modulation using a Tektronix TDS-520A digitizing oscilloscope. The time resolution of the spectrometer is in the 40−100-ns range. Tr-EPR signals in direct detection mode have a nonderivative line shape with enhanced absorptive (A) and emissive (E) electron-spin polarization. A complete data set consists of a series of transient signals taken at equidistant magnetic-field points covering the total spectral width. For improved signal-to-noise ratio, typically 25 transients were accumulated at each value of the magnetic field. Transient spectra can be extracted from this data set at any desired time after the laser pulse as slices parallel to the magnetic-field axis.
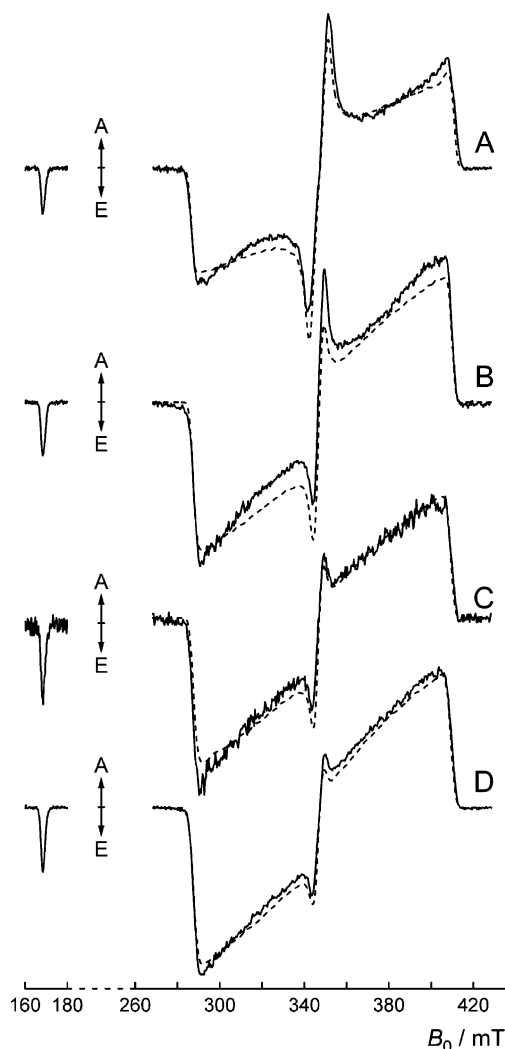
Optical excitation of the protein samples was achieved by a Nd: YAG (neodymium yttrium/aluminum garnet) laser pumped dye laser BMI AL.152C (Thomson-CSF, Buyancourt, France) with a wavelength of 440 nm (laser dye, coumarin-120), a pulse duration of $\sim$6 ns, a pulse energy of 1 mJ, and a laser repetition rate of 1 Hz.

Simulation of EPR Spectra. The EPR powder spectra have been analyzed using a program for simulation and fitting of spectra with isotropic *g*-factor and dipolar-coupling tensor **D** as described previously.[35]

Optical Spectroscopy. Low-temperature optical absorption spectra were measured with a Cary 1E spectrophotometer using a laboratory-built cryostat and an Oxford ITC-4 (Oxford Instruments, Oxford, UK) temperature controller with liquid nitrogen as coolant. The samples were illuminated with a filtered (410−480 nm) halogen lamp. The data were analyzed using singular value decomposition (SVD)[36,37] to deconvolute multiple overlapping spectra which developed in response to optical sample excitation.

Results

EPR Spectroscopy. The transient EPR spectra of various photoexcited wild-type LOV1 and LOV2 domains in frozen aqueous solution (T = 80 K) are shown in Figure 2. They were obtained from the magnetic-field-dependent EPR time profiles by integration over the time window of 500 ns centered at t = 1 μs after pulsed laser excitation. Each spectrum consists of a narrow emissively electron-spin polarized feature centered at $g \approx 4$ around 168.5 mT and a broad signal contribution centered

(35) Kowalczyk, R. M.; Schleicher, E.; Bittl, R.; Weber, S. *J. Am. Chem. Soc.* **2004**, in press (JA049554i).
(36) Shrager, R. I.; Hendler, R. W. *Anal. Chem.* **1982**, *54*, 1147.
(37) Hendler, R. W.; Shrager, R. I. *J. Biochem. Biophys. Methods* **1994**, *28*, 1.

Figure 2. Transient EPR spectra of various wild-type LOV domains in frozen aqueous solution measured at T = 80 K (solid lines). The spectra have been obtained from two-dimensional data sets $S(B_0, t)$ comprising of EPR time profiles measured at equidistant values of the magnetic field B_0. Each time profile is the average of 25 acquisitions recorded with a laser-pulse repetition rate of 1 Hz. For the spectra shown, the signal intensity of each time trace was integrated over a time window of 500 ns centered at 1 μs after pulsed laser excitation. Other parameters: microwave frequency, 9.68 GHz; microwave power, 25 dB (0.63 mW); detection bandwidth, 100 MHz. (A) wild-type LOV1 domain of *C. reinhardtii* fused to maltose-binding protein, (B) wild-type LOV2 domain of *A. capillus-veneris*, (C) wild-type LOV2 domain of *A. sativa* fusion protein with hisactophilin (HA), and (D) wild-type LOV2 domain of *A. sativa*. The dashed lines represent spectral simulations using the parameters given in Table 1.

at $g \approx 2$ in the magnetic-field range 280 mT $< B_0 <$ 410 mT with emissive electron-spin polarization below $g \approx 2$ and enhanced absorptive electron-spin polarization above $g \approx 2$.

The widths of the EPR spectra, the spectral positions of extrema and inflection points, and the overall polarization patterns are characteristic for photoexcited FMN triplet states generated by ISC from an excited singlet-state precursor.[35] The narrow lines at 168.5 mT are the so-called half-field transitions arising from formal "$\Delta M_S = \pm 2$" resonances between the lowest and highest energy levels in an intermediate magnetic-field regime in which the eigenfunctions of the spin Hamiltonian become linear combinations of the high-field states and $M_S \in \{-1, 0, +1\}$ are no longer adequate quantum numbers. In the past, using continuous-wave EPR with first-derivative detection

of the signal with respect to B_0 (as a consequence of magnetic-field modulation), observation of flavin triplets was mostly restricted to the "$\Delta M_S = \pm 2$" transition centered at $g \approx 4$ due to the high intensity of its first-derivative line.[38,39] The comparatively low intensity of the first derivative of the anisotropic and hence broad $\Delta M_S = \pm 1$ transitions in the range 280 mT $< B_0 <$ 410 mT and centered about $g \approx 2$ often precluded the observation of the complete flavin triplet signal. However, in an EPR experiment with sufficiently high time-resolution, which is for the first time performed here on FMN triplet states in a protein environment, the full electron-spin polarization of all transitions between the non-Boltzmann populated energy levels is exploited. Hence, a characteristic powder pattern is observed in which the $\Delta M_S = \pm 1$ transitions at the canonical orientations of the FMN triplet principal axes (X, Y, and Z) are separated by $|D'| + 3|E'|$, $|D'| - 3|E'|$, and $2|D'|$ (with $|D'| = |D| \, hc/(g\beta_e)$ and $|E'| = |E| \, hc/(g\beta_e)$), and centered about the g-value of the triplet.

Prior to a quantitative spectral analysis, the line shapes of all wild-type LOV domain spectra have been corrected for a partial, irreversible signal reduction that gradually progressed during the EPR signal accumulation over the entire magnetic-field range. The resulting line-shape distortions due to an exponential decay of the fraction of those FMN molecules which could be photoexcited into the triplet state were rectified by a two-step procedure (see also Supporting Information): (1) multiplication of the signal amplitudes $S(B_0)$ with a function $f(B_0)$ that compensates for the monoexponential decay of a fraction of photoactive FMN molecules, and (2) comparison of the resulting spectrum, $S(B_0) \times f(B_0)$, with that of an identically treated signal, $S'(B_0) \times f'(B_0)$, where $S'(B_0)$ was recorded in the opposite magnetic-field direction compared to $S(B_0)$ and corrected by multiplication with the corresponding function $f'(B_0)$. If $f(B_0)$ and consequently also $f'(B_0)$ are parametrized such that the normalized line shapes $S(B_0) \times f(B_0)$ and $S'(B_0) \times f'(B_0)$ are identical within experimental error, then $f(B_0)$ yields the fraction of irreversibly "lost" photoactive FMN molecules and also the exponential decay constant. For further discussion, however, the latter parameter is not used as it depends on the sample illumination conditions (laser pulse energy, sample excitation cross section) that may slightly vary in different experiments.

From the spectral line-shape-correction procedure, we found that for the wild-type *C. reinhardtii* LOV1 domain approximately $^1/_4$ of the sample gradually converted upon repetitive photoexcitation into a diamagnetic species that does not form a photoexcited singlet or triplet state by illumination with wavelengths around 440 nm and, hence, did not contribute to the triplet EPR spectrum of the FMN cofactor. In the various wild-type LOV2 domains, larger fractions were found to react irreversibly upon illumination. To clarify the origin of the decay of triplet-forming molecules, we performed additional low-temperature UV−vis experiments, which will be described below.

The spectral simulations of the corrected triplet EPR spectra yield the ZFS parameters, $|D| = |D'| \, g\beta_e/(hc)$ and $|E| = |E'| \, g\beta_e/(hc)$, and also the relative zero-field populations of the zero-field levels, p_X, p_Y, and p_Z, that are typically not obtained from a continuous-wave EPR experiment. The values for the different

(38) Shiga, T.; Piette, L. H. *Photochem. Photobiol.* **1964**, *3*, 213.
(39) Shiga, T.; Piette, L. H. *Photochem. Photobiol.* **1964**, *3*, 223.

Table 1. Triplet Zero-Field Splitting and Zero-Field Population Parameters of Free FMN in Frozen Aqueous Solution and FMN Cofactor Bound to Various Wild-Type and Mutant LOV Domains (T = 80 K) Obtained by Simulation of the Time-Resolved EPR Spectra of Figures 2 and 4[a]

	$|D|/(10^{-4} \, cm^{-1})$	$|E|/(10^{-4} \, cm^{-1})$	p_X	p_Y	p_Z
FMN	573	164	0.34	0.66	0
C. r. LOV1	581	167	0.68	0.32	0
Ad. LOV2	573	179	0.64	0.36	0
A. s. LOV2	570	181	0.62	0.38	0
A. s. LOV2 (−HA)	569	184	0.66	0.34	0
C. r. LOV1 C57S	598	158	0.54	0.46	0
A. s. LOV2 C450A	566	175	0.63	0.37	0

[a] Estimated error ranges for the $|D|$ and $|E|$ values are $\pm 6 \times 10^{-4}$ cm^{-1}, and for the zero-field populations (p_i), ± 0.03. *C. r.*, *C. reinhardtii*; *Ad.*, *A. capillus-veneris*; *A. s.*, *A. sativa*; HA, hisactophilin domain of *Dictyostelium discoideum*
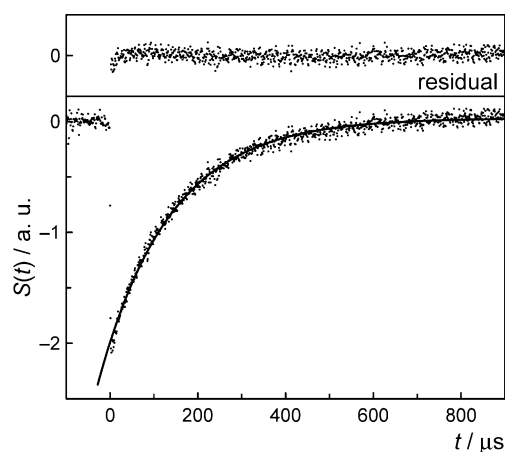
Figure 3. Time dependence of the transient EPR signal (dots) of the photoexcited triplet state of the FMN cofactor of *A. capillus-veneris* LOV2 recorded at 80 K (lower curve) at a magnetic field of 288.0 mT. The signal decay has been fitted with a monoexponential decay function (lower solid curve). The residuals are shown in the upper part. Other parameters: microwave frequency, 9.68 GHz; microwave power, 55 dB (0.63 μW); detection bandwidth, 100 MHz.

LOV domains are listed in Table 1 and compared with those from free FMN obtained under similar conditions.

For the FMN cofactors of all wild-type LOV samples, in particular for FMN bound to LOV2 domains, $|E|$ values larger than the one of free FMN in aqueous solution are observed. The corresponding $|D|$ values are, however, slightly smaller (LOV2) or somewhat larger (LOV1) than that of free FMN. Within experimental error, the same ZFS parameters are observed for *A. sativa* LOV2 domains, regardless of whether the hisactophilin (HA) domain fused to the LOV domain for increasing the protein solubility is present or not.

The relative zero-field populations, p_X and p_Y, are reversed in LOV domains compared to those of free FMN. This indicates that specific protein−cofactor interactions alter the symmetry of the triplet state such that the sign of E of protein-bound FMN is opposite to that of FMN in aqueous solution.

A characteristic EPR time trace showing the formation and the decay of the triplet EPR signal of FMN bound to the LOV2 domain of *A. capillus-veneris* is depicted in Figure 3. Similar EPR time traces were obtained for all other wild-type LOV domains (data not shown). The signal rise time is limited by the instrumental time response of the spectrometer, which is in the range of 40−100 ns. The exponential decay of the electron-

Table 2. Effective EPR Signal Decay Times of the Triplet State of Free FMN in Frozen Aqueous Solution and FMN Bound to Various Wild-Type and Mutant LOV Domains (T = 80 K) Obtained by Fitting of the Respective EPR Time Profiles with Monoexponential Decay Functions[a]
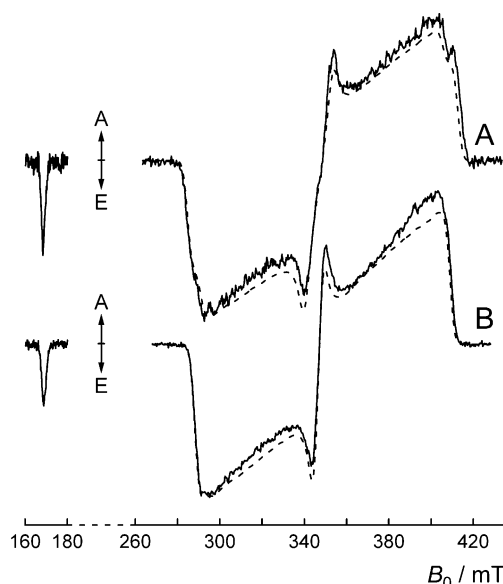
	$T_1/\mu s$
FMN	160
C. r. LOV1	148
Ad. LOV2	164
A. s. LOV2	178
A. s. LOV2 (−HA)	158
C. r. LOV1 C57S	169
A. s. LOV2 C450A	170

[a] The values are accurate to within 5% (abbreviations same as those in Table 1).

spin polarization of the triplet toward Boltzmann equilibrium is governed by spin relaxation. For very low microwave power, the effective decay time can be identified with the spin−lattice relaxation time T_1.[40] It should be noted, however, that the FMN triplet lifetime is typically much longer than the effective EPR signal decay time constant discussed here.[41−44] Due to the sensitivity loss as a consequence of the direct signal detection in tr-EPR, a relaxed triplet state in Boltzmann equilibrium is usually not visible by this technique, and therefore, information on the triplet lifetime cannot be given. For all FMN cofactor triplet states, the effective EPR signal decay time constants are comparable to that of free neutral FMN in aqueous solution. The signals decayed with time constants ranging from about 150 to 180 μs (see Table 2).

The photogenerated triplet EPR spectra of two LOV mutants, C57S of *C. reinhardtii* LOV1 and C450A of *A. sativa* LOV2, have also been recorded and are shown in Figure 4. The mutant LOV domains did not show a significant decay of the triplet intensity during signal accumulation. The spin-polarized triplet decay time constants are similar to those of the wild-type LOV domains (see Table 2). While the ZFS parameters $|D|$ and $|E|$ of LOV2 C450A resemble those of the other LOV2 domains, significantly different values have been obtained from spectral simulation of the triplet spectrum of LOV1 C57S (see Table 1). Also the zero-field population parameters of the LOV1 mutant differ from the values of the wild-type LOV1 and LOV2 domains.

UV−vis Spectroscopy. To further analyze the reason for the gradual reduction of the amplitude of the EPR signal during spectrum acquisition of the FMN triplets in photoexcited wild-type LOV domains, low-temperature optical absorption experiments on several wild-type and mutant LOV proteins were performed (see Figure 5). The samples were prepared under exactly the same buffer conditions as those that have been used to collect the EPR data (see above). The temperature range was also chosen to obtain comparable data. The optical absorption spectrum of wild-type LOV1 recorded at T = 77 K is shown in panel A of Figure 5 (solid line). The basic absorption properties

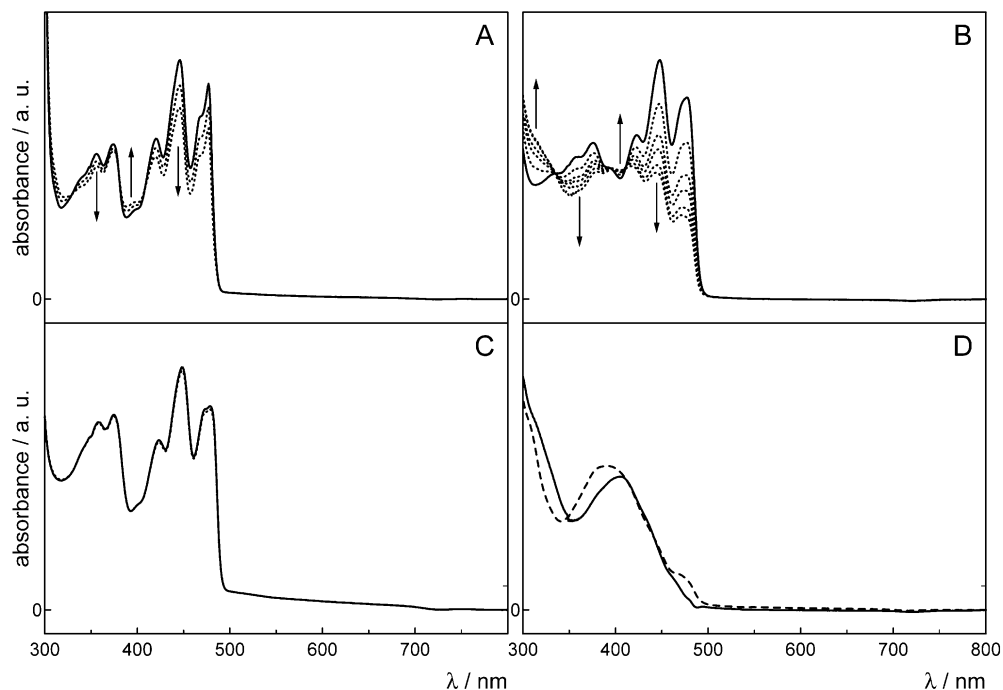(40) Atkins, P. W.; McLauchlan, K. A.; Percival, P. W. *Mol. Phys.* **1973**, *25*, 281.
(41) Moore, W. M.; McDaniels, J. C.; Hen, J. A. *Photochem. Photobiol.* **1977**, *25*, 505.
(42) Moore, T. A.; Kwiram, A. L. *Biochemistry* **1974**, *13*, 5403.
(43) Sun, M.; Moore, T. A.; Song, P.-S. *J. Am. Chem. Soc.* **1972**, *94*, 1730.
(44) Fritz, B. J.; Matsui, K.; Kasai, S.; Yoshimura, A. *Photochem. Photobiol.* **1987**, *45*, 549.

Figure 4. Transient EPR spectra of mutant LOV domains measured at 80 K (drawn lines). The spectra have been obtained as those shown in Figure 2. (A) *C. reinhardtii* C57S LOV1 domain. (B) *A. sativa* C450A LOV2 domain. The dashed lines represent spectral simulations using the parameters given in Table 1.

of LOV1 have been reported before.[45] The absorption bands centered at 446 and 356 nm represent the $S_0 \rightarrow S_1$ and $S_0 \rightarrow S_2$ transitions of the FMN cofactor, respectively. They exhibit an intense vibronic fine structure that is indicative of tight and well-defined binding between the noncovalently bound FMN and the highly ordered protein structure. Compared to previously published room-temperature data,[11,12] the low-temperature spectrum presented here shows improved spectral resolution. This is due to the reduction of protein motion at low temperature in frozen aqueous solution compared to that in liquid aqueous solution.

Irradiation of wild-type LOV1 at T = 77 K with blue light (410 nm < λ < 480 nm) leads to a partial bleaching of the absorption bands around 446 and 356 nm as shown in Figure 5 (panel A). The spectra shown have been recorded before illumination (solid line) and after illumination times of 16, 350, and 850 s (dashed lines). At 77 K, the observed bleaching shows virtually no recovery within a period of 12 h. Concomitant with the decrease in absorption around 356 and 446 nm, the absorption around 395 nm is increased (see below). After an extended period of illumination, about $^3/_4$ of the sample remained unaltered, whereas about $^1/_4$ of the sample decayed into the species absorbing at around 395 nm. Upon warming of the sample above the glass-transition temperature of the water/glycerol mixture, the decay back to the ground state, LOV-447, occurs on a time scale of minutes.

Similar results have been observed for wild-type LOV2 as shown in Figure 5 (panel B). The spectra shown have been recorded before illumination (solid line) and after illumination times of 3, 6, 9, 20, and 100 s (dashed lines). In contrast to the LOV1 sample, a larger fraction of LOV2-447 decays upon illumination (approximately $^2/_3$) into a species with an absorption maximum again around 400 nm (see also below). To exclude the possibility that this photoproduct arises from degradation

(45) Holzer, W.; Penzkofer, A.; Fuhrmann, M.; Hegemann, P. *Photochem. Photobiol.* **2002**, *75*, 479.

Figure 5. Photobleaching of wild-type (panels A and B) and mutant (panel C) LOV domains at $T = 77$ K. The solid lines in panels A−C represent the initial dark spectra, LOV1-447 (A), *A. sativa* LOV2-447 (B), and *A. sativa* LOV2-C450A-447 (C). Panel A: Absorbance changes measured for *C. reinhardtii* LOV1. The dotted lines represent spectra recorded after 16, 350, and 850 s of blue-light illumination. Panel B: Absorbance changes measured for wild-type *A. sativa* LOV2. The dotted lines represent spectra recorded after 3, 6, 9, 20, and 100 s of blue-light illumination. Panel C: Absorbance changes measured for *A. sativa* LOV2 C450A mutant. The dotted line represents the spectrum recorded after 1000 s of blue-light illumination. Panel D: The solid line represents the calculated optical absorption spectrum of wild-type LOV2-405 obtained by singular-value decomposition of the spectra of panel B. The dashed line shows the optical absorption spectrum of LOV2-390 generated at room temperature prior to freezing.

of the LOV2 domain's FMN cofactor, we have performed a similar experiment on a mutant *A. sativa* LOV2 domain, in which the photoreactive cysteine has been replaced by alanine (C450A). The cysteine-to-alanine replacement renders the LOV domain incapable of undergoing photoadduct formation while the triplet quantum yield and the ISC rate are only moderately altered as compared to the wild-type.[23] Here, only a negligible fraction of the sample (less than 2%) decays irreversibly (see Figure 5C). The major fraction, however, remains with unaltered optical absorption properties even after extended illumination conditions. This shows that the FMN cofactor bound to the LOV2 domain is photostable in the frozen state, a conclusion also consistent with the tr-EPR data on LOV2 C450A where no decay of the triplet intensity during signal accumulation has been observed. Based on these findings we can exclude an unspecific photodegradation of the wild-type LOV domains in the EPR experiments at low temperatures and assign the observed reduction of the triplet intensity in the tr-EPR experiments to the formation of a diamagnetic low-temperature adduct.
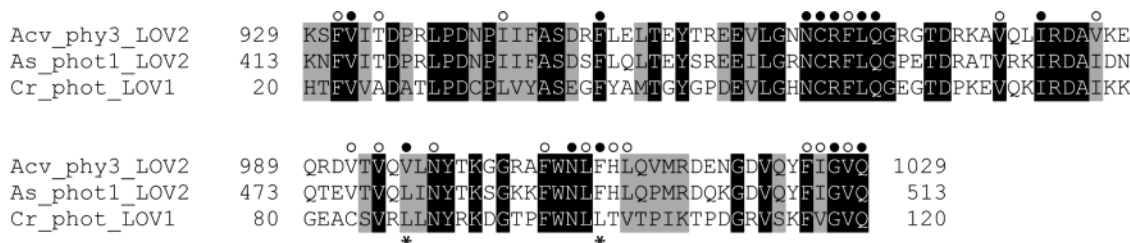
We have analyzed the wild-type LOV data using an SVD procedure.[36,37] This method allows the extraction of the spectrum of the photoproduct even in the case when it strongly overlaps with that of the dark state, LOV-447. The obtained result is unique if one assumes that the photoproduct spectrum must be positive at all wavelengths and should not contain the absorption maximum at 477 nm as does the dark state. The spectrum obtained in this way from the LOV2 data shows a broad absorption peaking at 405 nm without vibrational structure (solid line in panel D of Figure 5). The spectrum of this photoproduct (termed LOV2-405 here) resembles that of the photoadduct,

LOV2-390[12] (see Figure 1), occurring after illumination of wild-type LOV2 domains in liquid aqueous solution. For a better comparison with the spectrum of LOV2-405 in frozen solution, we generated the LOV2-390 photoadduct in liquid solution and shock-froze this sample to 77 K (dotted line in panel D of Figure 5). The spectrum shows an absorption maximum at 392 nm which is blue-shifted compared to the spectrum of LOV2-405 obtained by illumination of LOV2 at 77 K. Similar results were obtained for wild-type LOV1 (data not shown); however, the absorption maximum of the spectrum of the photogenerated low-temperature species is at about 390 nm. Again, the peak absorbance of the photoproduct generated by illumination at room temperature[12] at 380 nm is blue-shifted compared to that of the low-temperature photoadduct.

It is interesting to note that the apparent time scale for the low-temperature adduct formation follows the trend observed at room temperature. In the low-temperature experiments with LOV2, about 50% of the photoconversion is completed within 6 s, whereas the same turnover requires about 16 s in LOV1 (see panels A and B of Figure 5). This is in line with the generally higher room-temperature reaction rates reported for photoproduct formation in LOV2 domains as compared to LOV1 domains.[12,20] A quantitative discussion of this finding would require time-resolved optical absorption experiments at low temperatures, which is beyond the scope of this contribution.

Discussion

We have presented the spin-polarized EPR spectra of the FMN triplet states of various photoexcited LOV domains measured for the first time by direct-detection tr-EPR. Recording the signal amplitude at 1 μs after laser-flash excitation ensures

```
Acv_phy3_LOV2   929   KSFVITDPRLPDNPIIFASDRFLELTEYTREEVLGNNCRFLQGRGTDRKAVQLIRDAVKE
As_phot1_LOV2   413   KNFVITDPRLPDNPIIFASDSFLQLTEYSREEILGRNCRFLQGPETDRATVRKIRDAIDN
Cr_phot_LOV1     20   HTFVVADATLPDCPLVYASEGFYAMTGYGPDEVLGHNCRFLQGEGTDPKEVQKIRDAIKK

Acv_phy3_LOV2   989   QRDVTVQVLNYTKGGRAFWNLFHLQVMRDENGDVQYFIGVQ   1029
As_phot1_LOV2   473   QTEVTVQLINYTKSGKKFWNLFHLQPMRDQKGDVQYFIGVQ    513
Cr_phot_LOV1     80   GEACSVRLLNYRKDGTPFWNLLTVTPIKTPDGRVSKFVGVQ    120
```

Figure 6. Multisequence alignment of phototropin wild-type LOV domains from various organisms. Residues within a distance of 0.7 nm apart from the C(4a) carbon of the respective FMN cofactor in the *A. capillus-veneris* phy3 LOV2 crystal structure are marked with filled circles. Residues that are within 0.9 nm are marked with open circles. Conserved amino acid residues are shaded in black; similar residues (in electronic properties) are shaded in gray. Dissimilarities between residues in the LOV1 and LOV2 domains that are found within 0.7 nm from C(4a) of FMN are marked with asterisks. Acv_phy3_LOV2, *A. capillus veneris* (maidenhair fern) phy3 (BAA36192); As_phot1_LOV2, *A. sativa* (oat) phot1 (AAC05083); Cr_phot_LOV1, *C. reinhardtii* phot (CAC94940).

that the spectral shapes are not distorted by relaxation, e.g., by anisotropic T_1 or ISC. EPR spectroscopy of triplet states can provide information regarding the delocalization of the wave function. The ZFS parameters, D and E, are related to the overall distribution of the two-center spin contributions from the triplet state. The D value permits an estimate of the extent as well as the geometrical shape of the spin distribution through its distance dependence, $D \propto \langle (r^2 - 3z^2)/r^5 \rangle$, where r is the magnitude of the distance between the two unpaired electrons in the triplet state, and x, y, and z are the distances between spin centers projected onto the principal axes system of the molecule. The brackets $\langle ... \rangle$ denote the average over the electron distribution. For an oblate spin distribution, as one would expect for a planar aromatic molecule, D is positive.[46] The ZFS parameter $E \propto \langle (y^2 - x^2)/r^5 \rangle$ permits an assessment of the in-plane spin anisotropy. The sign of E is rather arbitrary, since interchanging the x and y axes reverses the sign of E.

Photogenerated Triplet States of Wild-Type and Mutant LOV Domains. Only small differences are found when the ZFS $|D|$ parameter of the triplet state of various wild-type LOV1 and LOV2 domains is compared to that of photoexcited FMN in frozen solution.[35] This indicates that the protein surroundings of the FMN cofactor in LOV domains do not drastically affect the electronic properties of the FMN triplet but rather provide a favorable spatial arrangement of the FMN cofactor relative to the photoreactive cysteine residue to facilitate adduct formation. On the other hand, although the ZFS $|E|$ values of free FMN and FMN bound in LOV domains are small in magnitude, by considering the zero-field populations, it is obvious that the sign of E is reversed in the flavoproteins compared to free FMN. This shows that the protein, by specific protein−cofactor interactions, alters the in-plane symmetry of the triplet wave function. The E parameter, however, is not easily interpreted and the computation of the sign and magnitude of D and E by quantum-chemical calculations remains difficult,[47,48] so in the following we will restrict ourselves to a qualitative discussion of the changes of D observed in the spectra.

(1) No changes of the ZFS parameters $|D|$ and $|E|$ have been observed between the *A. sativa* wild-type LOV2 proteins with and without attached HA domains. This implies that the electronic structure of the FMN triplet state is unaffected by changes at the surface of the LOV domain.

(2) The slightly different $|D|$ values observed for wild-type LOV1 and LOV2 domains compared to free FMN may be

understood in terms of the changes in the electronic structure of the cofactor induced by the protein, an effect often observed in optical spectroscopy. The slightly larger value of $|D|$ in LOV1 domains when compared to that of free FMN points at a more confined triplet state (see above), which might be induced by hydrogen bonds between the isoalloxazine moiety and the protein. On the other hand, the values of $|D|$ in LOV2 domains are very similar to that of free FMN; i.e., the triplet in LOV2 is more delocalized than that in LOV1. It would be expected that subtle variations in the electronic structure of the respective FMN cofactors are caused by the differences in the local environments of FMN in the LOV1 and LOV2 domains. We reproduce a protein alignment for the amino acid sequences of LOV1 and LOV2 for the organisms examined in this study in Figure 6. Within a 0.7-nm distance to C(4a) in the isoalloxazine moiety of FMN, algal LOV1 and fern and oat LOV2 differ at residues L87/V996/L480 (*C. reinhardtii* LOV1/*A. capillus-veneris* LOV2/*A. sativa* LOV2) and L101/F1010/F494. The replacement of leucine with the highly similar valine is not expected to cause any significant alteration of the FMN triplet wave function in LOV domains. However, the aromatic amino acid phenylalanine in LOV2 domains may well participate in partial triplet delocalization via π-stacking interactions with the central ring of the isoalloxazine moiety of FMN. A closest distance between these moieties of less than 0.3 nm is found from the X-ray crystal structure of *A. capillus-veneris* LOV2.[27] Triplet delocalization over a wider spatial range is expected to increase the average distance between the two spin centers in the triplet and thus decreases the magnitude of the ZFS parameter $|D|$. In algal LOV1, triplet delocalization does not occur; rather there is only some hydrophobic interaction between the leucine residue and the FMN cofactor.

Whether the slightly enhanced triplet delocalization in LOV2 can be related to its higher yield of adduct formation compared to LOV1 is a question that deserves further investigation. Mutating the phenylalanine in LOV2 to leucine, however, seems not to have a large effect on the relative quantum efficiency and dark-regeneration rate.[20]

(3) Since the slightly different protein surrounding of the FMN cofactor in LOV1 and LOV2 domains causes differences in the triplet parameters $|D|$ and $|E|$, it is not surprising that mutations in the binding site of the cofactor, e.g., LOV1 C57M or LOV2 C450A, also influence the electronic structure of the photoexcited FMN chromophore. Variations of the zero-field splitting parameters reflect the different polarities and hydrogen-bonding capabilities of the amino acids replacing the cysteine in the respective mutants.

(46) Hornig, A. W.; Hyde, J. S. *Mol. Phys.* **1963**, *6*, 33.
(47) Zuclich, J. *J. Chem. Phys.* **1970**, *52*, 3592.
(48) Havlas, Z.; Michl, J. *J. Chem. Soc., Perkin Trans. 2* **1999**, 2299.

Low-Temperature Photoreaction of Wild-Type LOV Domains. Iwata and co-workers have recently reported that LOV2 from *Adiantum* Phy3 undergoes thioadduct formation even at temperatures as low as 77 K.[49] Their conclusions are based on the disappearance of the characteristic S−H vibration band at around 2568 cm^{-1} in the Fourier transform IR spectra observed upon illumination in a temperature range from 77 to 295 K. Light-minus-dark difference optical absorbance spectra have also been presented; however, no spectrum of the "pure" thiophotoadduct has been shown. We report here unambiguous spectroscopic evidence for low-temperature photoadduct formation in *A. sativa* LOV2 and *C. reinhardtii* LOV1. We found that the respective photoreactions are not quantitative but rather proceed for fractions of up to 22% and 68%, respectively. Even after prolonged illumination times, considerable fractions of the wild-type LOV domains remain unaltered in the LOV-447 state.

The observation that only a fraction of all wild-type LOV domains reacts to the photoadduct species can be explained by a heterogeneous protein conformation in which the functional cysteine side chain assumes specific orientations with respect to the FMN cofactor: one, in which the sulfur of cysteine is in sufficient proximity to react with FMN in the triplet state, and another, where the sulfur is in an unfavorable position to react. Two such conformations, 1 and 2, have been observed in wild-type LOV1 from *C. reinhardtii* by low-temperature X-ray crystallography.[18] In the conformation 1, the cysteine sulfur is located above the planar 7,8-dimethyl isoalloxazine moiety of FMN, close to C(5a). In conformation 2, the thiol group of cysteine is rotated such that it is closer to C(4a) at a distance more favorable for covalent bond formation. Quantum-chemical calculations on these ground-state protein conformations have predicted that their energies differ by 0.4 kcal/mol.[18] The conformation 2 where the cysteine sulfur is closer to C(4a) has the lower energy. If the activation barrier for the conversion of these two conformations is too high to overcome at 77 K, then only conformation 2 could react to form the photoproduct species LOV-405. The ratio of the two conformations (70:30 = conformation 1/conformation 2) in the LOV1 structure[18] correlates reasonably well with the amount of low-temperature photoproduct observed by optical spectroscopy and tr-EPR. For *A. capillus-veneris* LOV2, the occurrence of two subspecies similar to the ones in LOV1 has not been reported.[27] That X-ray structure, however, was determined at room temperature and at considerably lower resolution. Hence, the two conformations might either not be distinguishable or their relative populations are shifted at low temperature more toward the configuration with the sulfur closer to C(4a) (conformation 2 in LOV1). The latter possibility is consistent with the larger fraction of photothioadduct formed in the LOV2 domains.

The optical absorption spectrum of the photogenerated LOV2-405 species was obtained by SVD and is presented in panel D of Figure 5. The shape of the spectrum strongly resembles that of the thiophotoadduct, LOV2-390, generated at room temperature and subsequently recorded after cooling to 77 K. However, the absorption maximum of LOV2-405 is red-shifted by 15 nm, revealing some structural dissimilarity compared to LOV2-390. Possible pathways for the formation of these species are shown in Figure 7 and are discussed below.

In all suggested reaction mechanisms, ISC of the FMN cofactor follows blue-light excitation both at room temperature and at 77 K to form the triplet state of FMN, ^{3}FMN (species A of Figure 7). Initially, it has been suggested that protonation of ^{3}FMN is a prerequisite to thioadduct formation, as it is thought to render the C(4a) position of FMN more electrophilic, thus enhancing the nucleophilic attack of the cysteine's thiol group on C(4a) (see species B of Figure 7).[13] The opposite effect, however, was reported from flash-photolysis experiments that probed the reactivity of flavin triplets with amino acids in aqueous solutions of different proton concentrations.[28] Cysteine was found to be more than 10-fold more reactive with ^{3}FMN than with ^{3}FMNH$^+$. If protonation of the FMN triplet would have occurred in the LOV domains prior to adduct formation at 77 K, then the resulting ^{3}FMNH$^+$, species B, would have been visible in the tr-EPR spectra. It would have been easily distinguished from ^{3}FMN by its ZFS parameters, $|D|$ and $|E|$, and also by its triplet relaxation time. These effects are not observed in the wild-type LOV domains, which rules out the presence of ^{3}FMNH$^+$ as an intermediate at 77 K. This finding is also in line with tr-EPR experiments on FMN in frozen aqueous solution, which have shown that proton transfer to ^{3}FMN does not occur at 77 K even when the chromophore is exposed to a glassy medium at pH 2.8 which is well below the pK_a of 4.4 as determined by optical spectroscopy for the protonation of ^{3}FMN.[35,50−52]

Considering an electron transfer from the functional cysteine to ^{3}FMN as suggested earlier[31,32] implies generation of a radical-pair species C and subsequently, following triplet-to-singlet conversion, the zwitterionic species D. Such a proposal is consistent with previous reports on the photoreactivity of FMN with amino acids in aqueous solution where evidence for a radical mechanism was presented if the photoreaction proceeds via the FMN triplet state.[28,53] As proton transfer, which is a necessary prerequisite for the formation of species E from species D, is drastically slowed if not completely inhibited at 77 K,[35] the primary photoadduct D would be expected to accumulate under these conditions. Species D formally carries a negative charge at N(5) of FMN and is protonated at the sulfur. The frequency position of the S−H vibration in an IR experiment should therefore be strongly shifted compared to that in LOV2-447 (species A) due to the trivalent sulfur binding situation in the adduct. This would account for the disappearance of the 2568-cm^{-1} band reported in the FT-IR studies by Iwata and co-workers.[49] The different charge distribution in species D as compared to that in LOV2-390 would also lead to an electrochromic shift of the low-temperature thioadduct optical absorption, which is observed experimentally (see Figure 5D).

If, however, adduct formation at low temperature were to proceed via hydrogen-atom transfer from the cysteine to the FMN (which in the glassy state would occur via quantum-mechanical tunneling to yield species F), then one would expect that the photoadduct species E should accumulate following triplet−singlet conversion. The optical absorption characteristics of this species would only differ from that of LOV2-390 if at

---

(49) Iwata, T.; Nozaki, D.; Tokutomi, S.; Kagawa, T.; Wada, M.; Kandori, H. *Biochemistry* **2003**, *42*, 8183.

(50) Sakai, M.; Takahashi, H. *J. Mol. Struct.* **1996**, *379*, 9.
(51) Schreiner, S.; Steiner, U.; Kramer, H. E. A. *Photochem. Photobiol.* **1975**, *21*, 81.
(52) Schreiner, S.; Kramer, H. E. A. Influence of pH on flavins in the triplet state. In *Flavins and Flavoproteins*; Singer, T. P., Ed.; Elsevier Scientific Publishing Company: Amsterdam, 1976; p 793.
(53) Traber, R.; Kramer, H. E. A.; Hemmerich, P. *Biochemistry* **1982**, *21*, 1687.
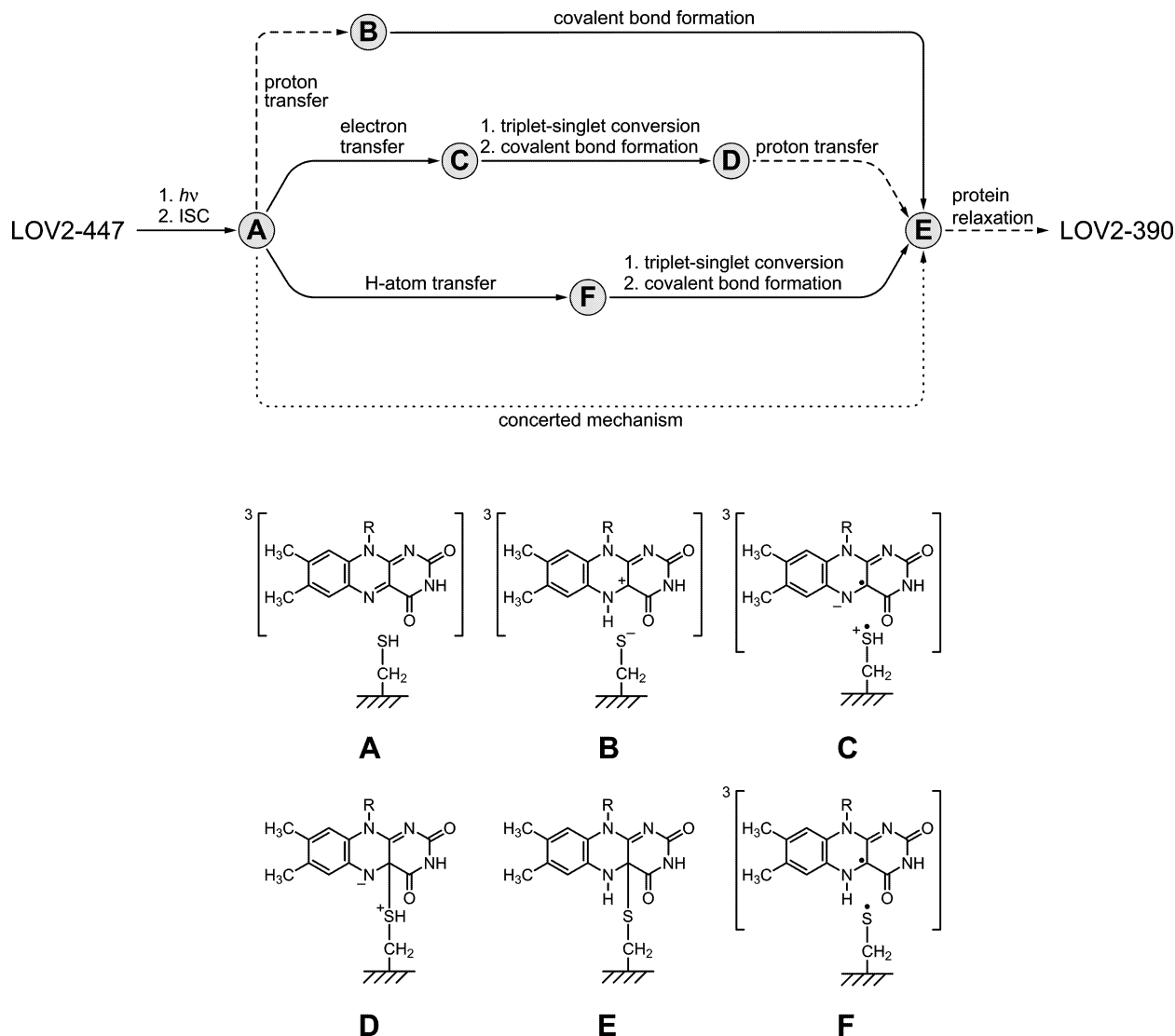
Figure 7. Suggested reaction pathway (top) and intermediates (bottom) of photoadduct (LOV-390) formation in wild-type LOV domains. Reaction steps that are inhibited at $T \leq 80$ K are shown with dashed arrows. For further details, see text.

low temperature the protein were unable to relax, thus imposing a conformational strain on the photoadduct. We consider that such a strain would be unlikely to cause the significant shifts observed in the optical absorption spectra (13 nm in LOV2 and 10 nm in LOV1), and hence we conclude that electron transfer is more likely than hydrogen-atom transfer if the photoadduct generation proceeds via radical-pair intermediates.

An alternative to the ionic and the radical-pair mechanisms discussed above is that the thioadduct, species E, is formed via a concerted mechanism, directly from the triplet state.[27] Such a mechanism requires either photoadduct formation in the triplet-spin configuration with subsequent triplet-to-singlet conversion or a direct transition from a photoexcited triplet precursor to a singlet product. However, we are not aware of any example of the latter reaction. A photoadduct species in the triplet state should in principle be observable by tr-EPR. No such additional paramagnetic species was observed in our experiments. Although it cannot completely be ruled out that the triplet of the adduct species might be hidden under the background of an excess of triplets from unreacted LOV domains, we consider the existence of such an intermediate as rather unlikely because

the triplet-state energy of the photoadduct is expected to be very high due to the formation of an sp³-hybridized C(4a) from a formerly delocalized (and hence stabilized) π-electron system in the FMN.

Conclusions

We have examined the photoreactivity of wild-type and mutant LOV domains by optical spectroscopy and time-resolved EPR at $T \leq 80$ K. The wild-type proteins still form an adduct via the photogenerated triplet state even at this nonphysiological temperature, although its optical absorption spectrum is slightly red-shifted from that observed in the usual adduct formed at ambient temperatures. No paramagnetic species other than the photogenerated triplet FMN have been observed, implying that adduct formation does not require prior protonation of triplet FMN.

Although a concerted mechanism for adduct formation cannot be completely ruled out by our experiments, we consider a radical-pair mechanism as the most likely mechanism for adduct formation at low temperature. As the oxidizing nature of ³FMN is virtually independent of the temperature, there is no reason

that the generation of the photothioadduct via an electron transfer is not active at ambient temperatures as well. The only difference between an electron-transfer mechanism at 77 K and at ambient temperatures is that the reaction step leading to a fully relaxed photoproduct is not inhibited under the latter conditions. Alternative mechanisms might also come into play at higher temperatures, but they will have to compete with electron transfer, which we consider unlikely.

We make these conclusions although a radical pair generated from ^{3}FMN and comprising an FMN radical anion and a sulfur-centered radical at the functional cysteine residue was not observed in the EPR experiments. There are several reasons for this, the most likely being that it reacts to form the adduct immediately after the initial triplet-state radical pair has converted to the singlet-state configuration and, hence, does not live long enough to be detected. Alternatively, and perhaps as well, because of the close proximity of the two radicals, their mutual dipolar and exchange interactions would be expected to broaden the resonance lines beyond detectability.

Although the structure of the low-temperature adduct could not be unequivocally determined, we propose that it is a zwitterionic adduct species with the thiol proton still bound to the sulfur atom. Time-resolved optical absorption spectroscopy and vibrational spectroscopy at low temperatures would be helpful for the determination of additional intermediate states during adduct formation in LOV domains. Such experiments could provide new insights into the mechanism of this fascinating signaling domain, which, most unusually, forms a covalent bond between its cofactor and an amino acid residue via the chromophore's photoexcited triplet state.

Supporting Information Available: A detailed description of the EPR line shape correction procedure used to account for the irreversible decay of a fraction of photoexcited LOV domains. This material is available free of charge via the Internet at http://pubs.acs.org.

JA049553Q